One-shot-phase-shifting Fourier domain optical coherence tomography by reference wavefront tilting

Yoshiaki Yasuno, Shuichi Makita, Takashi Endo, Gouki Aoki, Hiroshi Sumimura, Masahide Itoh and Toyohiko Yatagai

Institute of Applied Physics, University of Tsukuba, Tennodai 1-1-1, Tsukuba, Ibaraki, 305-8573, Japan

yasuno@optlab2.bk.tsukuba.ac.jp

URL: http://optics.bk.tsukuba.ac.jp/COG/

Abstract: A novel optical scheme for a phase shifting method of Fourier domain optical coherence tomography is presented. With this method we avoid a mechanical scan for phase shifting (mechanical M-scan) by using a reference beam with tilted wavefront. The principle of this system is confirmed with a simple mirror object. This method is applied on a biological sample and used to investigate a porcine anterior eye chamber.

OCIS codes: (110.4500) Optical coherence tomography, (100.2650) Fringe analysis, (170.4500) Optical coherence tomography, (120.3890) medical optics instrumentation

References and links

1. D. Huang, E. A. Swanson, C. P. Lin, J. S. Schuman, W. G. Stinson, W. Chang, M. R. Hee, T. Flotte, K. Gregory, C. A. Puliafito, J. G. Fujimoto, "Optical coherence tomography," Science **254**, 1178–1181 (1991).
2. Häusler G, Lindner MW, " "Coherence rader" and "spectral radar"—New tools for dermatological diagnosis," J. Biomed. Opt. **3**, 21–31 (1998).
3. Maciej Wojtkowski, Tomasz Bajraszewski, Piotr Targowski, Andrzej Kowalczyk, "Real-time in vivo imaging by high-speed spectral optical coherence tomography," Opt. Lett. **28**, 1745–1747 (2003).
4. R. A. Leitgeb, C. K. Hitzenberger, A. F. Fercher, "Performance of Fourier domain vs. time domain optical coherence tomography," Opt. Express **11**, 889–894 (2003), http://www.opticsexpress.org/abstract.cfm?URI=OPEX-11-8-889.
5. Y. Yasuno, S. Makita, Y. Sutoh, M. Itoh, and T. Yatagai, "Birefringence imaging of human skin by polarization-sensitive spectral interferometric optical coherence tomography," Opt. Lett. **27**, 1803–1805 (2002).
6. Yoshiaki Yasuno, Shuichi Makita, Takashi Endo, Masahide Itoh, Toyohiko Yatagai, Mari Takahashi, Chikatoshi Katada and Manabu Mutoh, "Polarization-sensitive complex Fourier domain optical coherence tomography for Jones matrix imaging of biological samples," Appl. Phys. Lett. **85**, 3023-3025 (2004).
7. Brian R. White, Mark C. Pierce, Nader Nassif, Barry Cense, B. Hyle Park, Guillermo J. Tearney, Brett E. Bouma, Teresa C. Chen, Johannes F de Boer, "*In vivo* dynamic human retinal blood flow imaging using ultra-high-speed spectral domain optical coherence tomography," Opt. Express **11**, 3490–3497 (2003), http://www.opticsexpress.org/abstract.cfm?URI=OPEX-11-25-3490.
8. Rainer A. Leitgeb, Leopold Schmetterer, Christoph K. Hitzenberger, Adolf F. Fercher, Fatma Berisha, Maciej Wojtkowski and Tomasz Bajraszewski, "Real-time measurement of in vitro flow by Fourier-domain color Doppler optical coherence tomography," Opt. Lett. **29**, 171-173 (2004).
9. Y. Yasuno, Y. Sutoh, M. Nakama, S. Makita, M. Itoh, T. Yatagai, and M. Mori, "Spectral interferometric optical coherence tomography with nonlinear β-barium borate time gating," Opt. Lett. **27**, 403–405 (2002).
10. M. Wojtkowski, A. Kowalczyk, R. Leitgeb and A. F. Fercher, "Full range complex spectral optical coherence tomography technique in eye imaging," Opt. Lett. **27**, 1415–1417 (2002).
11. E.g., J. E. Greivenkamp, J. H. Bruning, Daniel Malacara, *et al.*, "Optical Shop Testing," 2nd ed., A Wiley-Interscience Publication, Chapter 14, (1992).

#5726 - $15.00 USD Received 12 Nov 2004; revised 26 Nov 2004; accepted 29 Nov 2004

12. Joanna Schmit and Katherine Creath, "Extended averaging technique for derivation of error-compensating algorithms in phase-shifting interferometry," Appl. Opt. **34**, 3610–3619 (1995).
13. Andrew M. Rollins, Joseph A. Izatt, "Optimal interferometerdesigns for optical coherence tomography," Opt. Lett. **24**, 1484–1486 (1999).

1. Introduction

Optical coherence tomography (OCT)[1] has been employed for varieties of biomedical applications, e.g., endoscopic investigation of internal organs and investigation of a retina and an anterior chamber in ophthalmology. OCT is a version of dual beam low-coherence interferometer, which non-destructively reveals the details of samples, so it is appropriate for medical and biological investigation. In recent years, Fourier-domain OCT (FD-OCT)[2] has attracted great attention, because of its fast measurement time[3] and its higher signal-to-noise ratio (SNR) than conventional delay-based OCTs[4]. FD-OCT is an improved version of OCT, which acquires spectral interference fringes by a spectrometer and calculates a cross-sectional OCT image without mechanical depth-scans (A-scans). FD-OCTs have also been applied for polarization sensitive FD-OCTs[5, 6] and Doppler FD-OCTs[7, 8].

Although FD-OCT is a promising technology, an FD-OCT image is disturbed by a ghost image and auto-correlation signals of reference and probing beams. The ghost image comes from the cosine term of a spectral interference fringe and is a mirror-reversed complex conjugate image of an OCT image. To have a proper OCT image, we had to restrict the axial measurement range and separate these signals. However, this restriction reduces the depth measurement range in half. An optical method[9] and an optical signal processing method[10] have been proposed to overcome this difficulty. This optical signal processing method, namely phase-shifting FD-OCT, which acquires several, typically five, spectral fringes with different carrier phase offsets for one depth-scan (A-scan), reconstructs a complex spectrum including phase information, and eliminates the disturbing signals.

The phase-shifting algorithm, as mentioned above, requires multiple fringes with different phase offsets. The acquisition of these fringes requires an additional dimension of mechanical scanning of path-length difference (M-scan), resulting in longer measurement time. Several spectral fringes constructing one A-scan are measured at different times, so that the accuracy of the OCT is more affected by the vibration of the sample and the system itself than conventional OCTs.

In this Letter, we propose a new method to acquire several spectral fringes with different phase offsets enabling a phase-shifting algorithm simultaneously without a mechanical M-scan and which enables one-shot phase-shifting FD-OCT. This FD-OCT system uses a two-dimensional CCD camera for fringe detection. One axis of the CCD camera, we will call it the *x*-axis, is occupied with the optical spectral axis and the other, *y*-axis is employed for phase offset variation.

2. Method

To understand the technique, it is appropriate first to describe the experimental setup. Figure 1 shows the schematic setup of our phase shifting FD-OCT. The light source is a femtosecond pulse laser, which has 775 nm central wavelength and 150 fs duration resulting in 22 μm axial resolution. The incident beam is split by a beam splitter (BS) into a reference beam and a probing beam. The probing beam is focused on the sample to be investigated by an objective lens, is scattered and reflected, then is introduced into a spectrometer consisting of a grating, a cylindrical lens and a CCD camera. The focal length of the objective, 100 mm, indicates 49 μm maximum lateral resolution with the 2 mm-diameter of our probing beam. The reference beam is reflected by a reference mirror and then introduced into the spectrometer. These two beams

#5726 - $15.00 USD Received 12 Nov 2004; revised 26 Nov 2004; accepted 29 Nov 2004

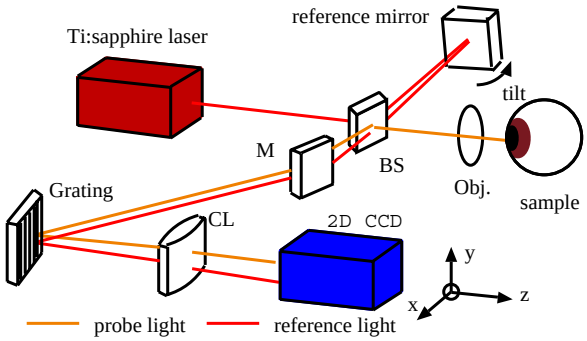

Fig. 1. The schematic diagram of the phase shifting Fourier domain OCT system. M; a mirror, BS; a beam splitter, Obj; an objective and CL; a cylindrical lens.

interfere with each other in a spectral domain and show a spectral interference fringe on the CCD as

$$\tilde{I}(\omega) = |\tilde{p}(\omega)|^2 + |\tilde{r}(\omega)|^2 + 2\,|\tilde{p}(\omega)|\,|\tilde{r}(\omega)|\cos\left(\omega\tau_d - \angle\tilde{p}(\omega) + \varphi\right) \tag{1}$$

where $\tilde{r}(\omega)$ and $\tilde{p}(\omega)$ are respectively the Fourier transforms of $r(t)$ and $p(t)$: temporal complex profiles of the reference beam and the probing beam. $\angle\tilde{p}(\omega)$ is the phase-angle of $\tilde{p}(\omega)$ and φ is the initial phase offset employed for the phase-shifting method described below. Here $p(t)$ contains the depth-structure of the sample in the manner of $t = 2z/v$ (v is the speed of light in the sample, z is the axial position). τ_d is the carrier frequency of this spectral fringe in proportion to the offset path-length difference between the reference path and probing path of the low-coherence interferometer.

Digital Fourier transform of the spectral fringe, Eq. (1), brings

$$\begin{aligned} I(\tau) = \Gamma[p(\tau)] + \Gamma[r(\tau)] + \left(\Gamma[p(\tau), r(\tau)]\, e^{i\varphi}\right) * \delta(\tau - \tau_d) \\ + \left(\Gamma[r(\tau), p(\tau)]\, e^{-i\varphi}\right) * \delta(\tau + \tau_d) \end{aligned} \tag{2}$$

where Γ and δ respectively represent the correlation-operation and a delta function. The 3rd and 4th terms of this equation, which come from the cosine term of Eq. (1), are a one-dimensional OCT signal denoting the depth structure of the sample and its mirror-reversed complex conjugate. Although this equation provides a one-dimensional OCT signal without a mechanical A-scan, it also contains the ghost signal and two auto-correlations of the reference beam and probing beam corresponding to the 1st and the 2nd terms of Eq. (2). The auto-correlation signals occupy the center of the signal field, namely the zero-delay point. The mirror-reversed ghost signal, which is superimposed on the substantial OCT signal, spoils the OCT measurement.

A reasonable way to divide these two signals is to restrict the depth measurement range to one-half. There is a trade off between the depth measurement range and the resolution in a FD-OCT, because of the limited number of the pixels of the CCD camera. Hence, the additional reduction of the measurement range by the ghost signal is a serious problem.

Phase-shifting FD-OCTs have been developed to overcome this problem. The phase-shifting FD-OCT, which acquires several spectral fringes with different phase offsets, reconstructs a complex spectrum by a phase shifting algorithm[11] and eliminates the ghost signal and auto-correlation signals. The reconstructed complex spectrum is described as

$$\tilde{I}_{ps}(\omega) = |\tilde{p}(\omega)|\,|\tilde{r}(\omega)|\exp i\left(\omega\tau_d - \angle\tilde{p}(\omega)\right). \tag{3}$$

#5726 - $15.00 USD Received 12 Nov 2004; revised 26 Nov 2004; accepted 29 Nov 2004

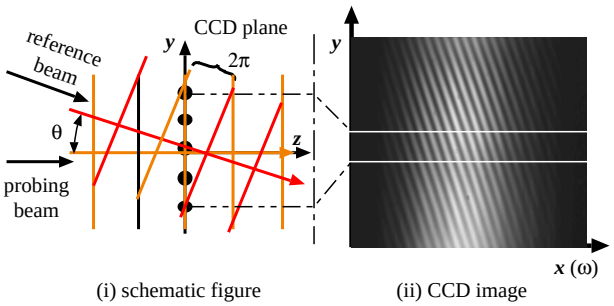

Fig. 2. Schematic figure of phase offset control by the tilt of reference wavefront (i), and one-shot spectral interferogram on CCD camera.

The digital Fourier transform of this signal results in

$$I_{ps}(\tau) = \Gamma[p(\tau), r(\tau)] * \delta(\tau - \tau_d). \tag{4}$$

Although it is clear that the phase shifting method has eliminated the disturbing signals, the variable phase offset requires an additional M-scan. Typically, additional mechanical scanning achieves the additional M-scan, but it extends the acquisition time and also reduces the vibration stability of the FD-OCT. In this Letter, we accomplish the additional M-scan without mechanical scanning in the following manner.

One will find the slight tilt of the reference mirror along the *y*-direction in our FD-OCT system described in Fig. 1. Although this system leads the reference beam into the spectrometer in parallel with the probing beam in the *x*-direction, these two beams have a different incident angle in the *y*-direction because of the *y*-tilt of the reference mirror. The schematic figure on the CCD plane, Fig. 2(i), shows that the *y*-axis on the CCD camera corresponds to the phase offset φ.

Figure 2(ii) shows a CCD image of spectral fringes. Its horizontal axis, namely the *x*-axis, depicts the optical frequency and its vertical axis, namely the *y*-axis, corresponds to the phase offset. This CCD image proves that several spectral fringes with different phase offsets exceeding a 2π-phase range have been acquired simultaneously with this one-shot measurement. This example is demonstrated with a plane mirror as a measured object, to clarify the effect of phase offset variation, but it is also applicable to more complex and practical objects as we will mention later.

Our phase-shifting FD-OCT system extracts five spectral fringes with phase offsets of $\varphi = 0, \pi/2, \pi, 3/4\pi, 2\pi$ and applies a 5-frame phase-shifting algorithm[12] to reconstruct a complex spectrum.

Figure 3(ii) shows the one-dimensional OCT signal of the plane mirror object calculated from the complex spectrum. As a reference, a one-dimensional OCT signal calculated from a non-complex spectral fringe measured from the same object is shown in Fig. 3(i). The signal in Fig. 3(i) consists of not only an OCT signal but also its conjugate ghost signal and two autocorrelation signals which overlap each other at the center of the field. In Fig. 3(ii), the disturbing conjugate signal and autocorrelations are absolutely eliminated and only the substantial OCT signal is shown.

We also note that, this FD-OCT system re-scaled the complex spectrum from wavelength scale to optical frequency scale before the digital Fourier transform to suppress depth-dependent signal attenuation.

#5726 - $15.00 USD
Received 12 Nov 2004; revised 26 Nov 2004; accepted 29 Nov 2004

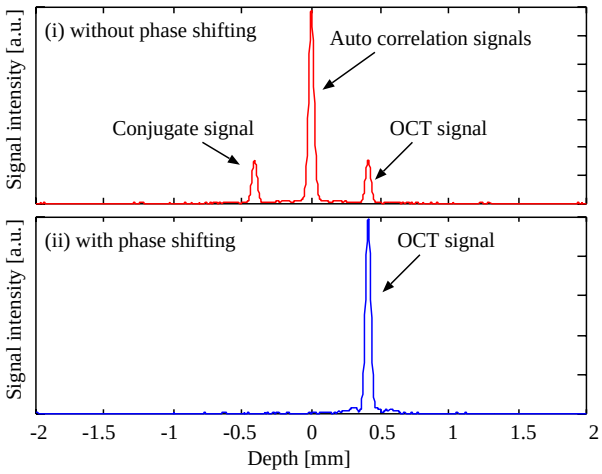

Fig. 3. One dimensional OCT signals measuring a mirror-surface, The signals represent a reconstructed signal without phase shifting (i) and with phase shifting (ii).

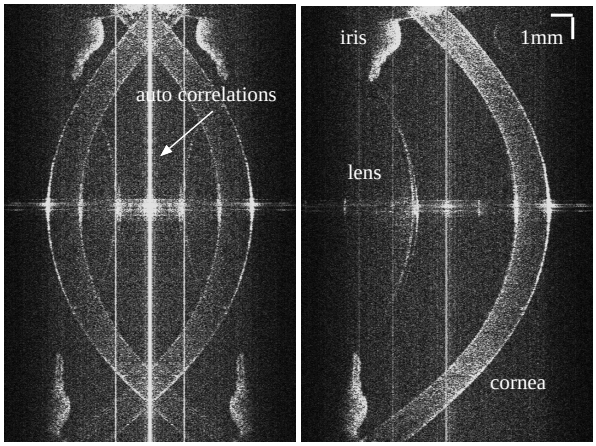

Fig. 4. Anterior chamber of on *ex-vivo* porcine eye. OCT images reconstructed without phase-shifting algorithm (i), and with phase-shifting algorithm (ii).

3. Measurement and results

Although we have not mentioned a lateral scan (B-scan) in the preceding description, this system also takes a two-dimensional OCT image with a B-scan. Figure 4 shows the cross-sectional OCT image of an *in vitro* porcine anterior eye chamber taken with a mechanical B-scan accomplished by a lateral scan of the sample stage. Figure 4(i) and 4(ii) respectively show OCT images without and with this phase-shifting method. In Fig. 4(ii), although we still find a remaining auto-correlation peak, its intensity has been remarkably attenuated and the ghost image, which we clearly see in Fig. 4(i), has also been eliminated. This result demonstrates that this wavefront-tilt-based phase shifting method is also applicable for biological samples.

#5726 - $15.00 USD
Received 12 Nov 2004; revised 26 Nov 2004; accepted 29 Nov 2004

4. Discussions

4.1. Phase calibration

The phase offsets, φ, of each row of the CCD camera are determined in a phase calibration process. In this process, we measure a 2D spectral interferogram with a plane mirror sample. Each row of the spectral interferogram are Discrete-Fourier-Transformed (DFT) and the phase value of the Fourier transformed signal peak is regarded as the phase offset of the corresponding row.

4.2. Wavelength dispersion and other phase-calculating algorithms

In the signal processing described in this letter, we have assumed that the phase offset induced by the variation of the path length difference, is independent of wavelength λ. However, the variation of the phase offset is described as

$$\varphi = 4\pi \frac{\delta L}{\lambda} \tag{5}$$

where δL is the variation of the path length difference. From Eq. (5), we find that φ is a function of λ.

In our method, the maximum variation of the path-length difference is $\delta L = \lambda_c/2$ corresponding to a 2π-modulation, where λ_c is the central wavelength. The λ_c is taken 775 nm for our light source. According to these equations, the maximum phase error is 0.097 rad, namely 1.5 % of 2π. The 5-frame phase-shifting algorithm is capable of compensating this amount of phase error[10, 12]. Even if we use a broader band light source and allow a larger phase error, we can apply a generalized least-squares phase shifting algorithm[11] for individual wavelength components independently. This algorithm eliminates the phase errors, although it is relatively time consuming.

A DFT applied to each column, namely each wavelength component, also could be used to retrieve the phases of each wavelength component. This technique gives a better signal to noise ratio due to averaging effect of DFT. However it is relatively time consuming and requires more data points than 5-frame phase-shifting algorithm. For example, five points required for our method, are not sufficient for this DFT method.

4.3. Signal-to-noise ratio and system speed

This FD-OCT system employs an 8-bit CCD camera with 640 lateral pixels for faster acquisition time and total cost reduction. Although this results in a relative low SNR of 46 dB without phase-shifting, the phase-shifting improves the SNR to 52 dB, twice the original SNR. This is because phase shifting algorithms summate substantial signals coherently, but merge noises incoherently.

Other simple methods, e.g., using a CCD camera which has the larger number of pixels, also enlarges the measurement range. However, complex FD-OCT systems, such as, our wavefront tilting method or path-length modulation method[10] have a certain advantage of signal-to-noise ratio in comparison to the other simple methods. We also note that, the complex FD-OCTs, in general, require relatively long acquisition time because they use several interference signals to construct the phase information.

Although the 2D CCD camera used in our system is a relatively slow device, the SNR-property of the phase-shifting might allow us to employ a CMOS camera which has low dynamic range but fast acquisition time to build a high-speed FD-OCT. For example, a 2D CMOS camera with 67 pix/sec data transfer rate has already been commercially available and this high-speed camera could result in 25 frames/sec movies of OCT images with 1024 (depth) $\times$ 512

#5726 - $15.00 USD Received 12 Nov 2004; revised 26 Nov 2004; accepted 29 Nov 2004

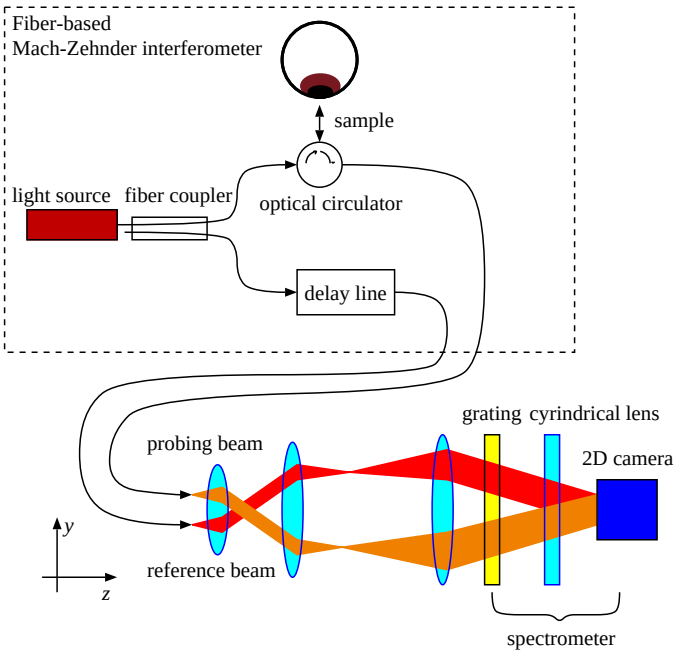

Fig. 5. An example of a fiber-based reference wavefront tilting FD-OCT system. The interferometer is a conventional fiber-based Mach-Zehnder interferometer, and the reference wavefront tilting is induced by the separation of two fiber tips.

(transversal) pixels. Our wavefront tilting method allows five-times-longer exposure-time than conventional phase-shifting FD-OCTs, since the five interferograms are acquired simultaneously. Thus the longer exposure time of our method compensates the low quantum efficiencies of the CMOS cameras.

4.4. Effect of comatic aberration

A cylindrical lens used in the spectrometer could induce a comatic aberration when the incident angles along *y*-axis are too large.

In our setup, the incident angle has been suitably minimized. Although the comatic aberration is clearly visible in coherent imaging system as an additional fringe pattern, Fig. 2(ii) does not show such additional fringes. It indicates that the comatic aberration is successfully eliminated in our system.

4.5. Fiber-based system

In this letter, a bulk FD-OCT system has been employed to implement the wavefront tilting method. However, this method can also be applied to fiber based FD-OCT systems. In this case, the interferometer of the FD-OCT system is nearly identical to a conventional fiber-based Mach-Zehnder OCT systems[13]. The wavefront tilting is induced by the separation between the probing and the reference fiber-tips along *y*-axis as shown in Fig. 5. Here the tilting angle between the probing and reference beams are proportional to the separation of these two tips.

#5726 - $15.00 USD Received 12 Nov 2004; revised 26 Nov 2004; accepted 29 Nov 2004

5. Conclusions

In conclusion, a phase-shifting FD-OCT system was demonstrated, which does not use a mechanical M-scan but instead a reference beam with a tilted wavefront. This method has been examined with a one-dimensional measurement. A two-dimensional OCT measurement of a porcine anterior eye chamber has been performed and revealed the interior structure of the sample. This FD-OCT system showed 52 dB SNR with a low-cost 8-bit CCD camera with 640 lateral pixels.

#5726 - $15.00 USD Received 12 Nov 2004; revised 26 Nov 2004; accepted 29 Nov 2004